

Molecular Docking, Synthesis and Determination of Anticancer Potential of Novel Pyrimidine Derivatives: *In vitro* and *in silico* Characterization

Machhindra Holam^{1,*}, Sunil Galatage², Supria Gaud¹, Sanika Kumbhar¹, Aishwarya Devaru¹, Saniya Inamdar¹, Sushma Dokare¹

¹Department of Pharmaceutical Chemistry, Sant Gajanan Maharaj College of Pharmacy, Mahagaon, Maharashtra, INDIA.

²Department of Pharmaceutics, Vasantidevi Patil Institute of Pharmacy, Kodoli, Maharashtra, INDIA.

ABSTRACT

Background: Lung and colon carcinoma are leading causes of mortality among all cancers and cases are increasing drastically. Chemotherapy plays vital role in the treatment of carcinoma and a new series of pyrimidine heterocycles attached to an azetidone has strong anti-cancer potential. **Aim:** Aim of current research work is to investigate the affinity of pyrimidine derivatives with the CDK4 protein using molecular docking. **Materials and Methods:** Antitumor activity of synthesized compounds was checked on HT29 and A549. The active site of the targeted protein identified by the help of docking techniques and the binding energies were calculated. Consequently, it was shown that compounds with docking scores of 6R, 6L and 6P have higher scores than those with scores in the series. **Results:** All the synthesized compounds were examined for GI_{50} , TGI and LC_{50} , while 6L and 6m showing predominant activity were tested for apoptosis. The compounds 6L and 6M exhibit the highest inhibitory activity on HT29 and A549 cell, the IC_{50} value of 10.0 and 17.2 $\mu\text{g/mL}$ are respectively. The compounds 6M and 6L found significant anticancer potential on HT29 and A549 respectively. Both synthesized compounds successfully induce apoptosis potential in HT29 and A549 cell lines, which is confirmed by flow cytometry and DAPI staining. **Conclusion:** in the present study synthesized pyrimidine derivatives represent a viable strategy for the development of a novel anticancer moiety with potent anticancer and apoptotic effects. However; further *in vivo* animal studies are required to establish its efficacy in the treatment of cancer.

Keywords: Anticancer, Apoptosis, CDK4, Molecular docking, Pyrimidine.

Correspondence:

Mr. Machhindra Holam

Department of Pharmaceutical Chemistry, Sant Gajanan Maharaj College of Pharmacy, Mahagaon, Maharashtra, INDIA.

Email: macholam10@gmail.com

Received: 27-05-2025;

Revised: 18-07-2025;

Accepted: 01-09-2025.

INTRODUCTION

Worldwide cancer is the leading cause of death and cases increasing drastically; approximately 19.3 million, recently nearly 10 million deaths in the year 2020 are due to cancer. The burden of cancer has significantly increased in the modern era. Female breast cancer projected 2.3 million new cases (11.7%). Next in line are malignancies of the lung (11.4%), colon (10.0%), prostate (7.3%) and stomach (5.6%).¹ The possible cancer treatment viz. Surgery, radiation, chemo and hormone therapy are available. The many factors influence the course of treatment.² According to GLOBACON up to 2040 the global cancer burden is projected to rise 47% compared to 2020 and rise in 28.4 million new cases. So, we need for therapeutic agents completely eradicate the cancer.

Drug repositioning is the most recently used tool for the identification of anticancer agents instead of *in vivo* synthesis. New indications for an already existing drug molecule will be discovered during the drug repositioning process for the treatment of other diseases. For example, sildenafil, which was initially developed as a c-GMP-specific phosphodiesterase-5 inhibitor, failed its II phase clinical trial for anti-anginal use. The drug's side effect, penile erection, was discovered in a clinical trial and sildenafil was then approved for use as a treatment for erectile dysfunction.³ On the other hand, the efficacy of drug repositioning is low, along with its ample adverse effects.⁴

Nowadays, the use of biomarkers for drug target identification and understanding of the mechanism of action improves the accuracy of anticancer agents. Various proteins, metabolic derivatives and immunological agents can be used as biomarkers for the development of efficient anticancer agents.⁵ The one-carbon metabolism pathway is an appealing target for development of new inhibitors target the cancer due its non-regulation in cancer cells.⁶ Targeting this pathway may reduce adverse drug effects,



DOI: 10.5530/ijper.20260733

Copyright Information :

Copyright Author (s) 2026 Distributed under Creative Commons CC-BY 4.0

Publishing Partner : Manuscript Technomedia. [www.mstechnomedia.com]

increase efficacy and overcome drug resistance in cancer cells. The development of anticancer drug greatest benefit in specific patient populations.⁷ One carbon metabolism, including serine hydroxy methyl transferase-2 and methylene tetrahydrofolate dehydrogenase-2, is a new target for the discovery of anticancer agents.⁸ Two compounds, MIT and MIN, were discovered by using a structure-based drug design method and showed good interactions with SHMT2 and MTHFD2 targets. Present research work aims to investigate the molecular docking, synthesis and evaluation of the anticancer potential of pyrimidine derivatives for cancer treatment.^{9,10}

MATERIALS AND METHODS

In silico Studies

The C-Docker protocol was used to conduct a molecular docking investigation using the Discovery Studio 2019 program. The Crystallographic enzyme (CDK2) substrate downloaded (PDB ID: 2A4L) from PDB. The protein structures were cleaned and verified for any missing atoms, bonds, or connections. Ligand was prepared in the required format and all annoying small molecule were deleted. A protein preparation wizard in macromolecules tools was used to prepare the receptor. Missing loops are first introduced and corrected using modeler if their lengths are less than or equal to the maximum loop length. CHARMM minimization was used for further refining chem3D version 18.1 was used to sketch up compound structures and MM2 reduction was carried out. Ligands were loaded and minimization performed using the CHARMM force field and steepest descent technique. By choosing the co-crystal ligand, the binding site was established. For docking studies, the CDOCKER technique was used. The "C-docker Energy" and "C-docker interaction energy" parameter were utilized for the determination of interaction. The strong positive value of those markers suggested that the ligands and receptor interacted well.¹¹

Docking Protocol Validation

We validated the adopted docking methodology to substantiate the dependability of the docking parameter system by performing the RMSD calculation between the docked pose and the crystal structure.

Chemistry

Step-I

The compound (2) was prepared by heating the benzaldehyde, 5.30 g. (0.1 mol), ethylcyanoacetate, 5.65 g (0.1 mol), thiourea, 3.80 g (0.1 mol) and anhydrous K₂CO₃, 6.91 g (0.1 mol) in absolute ethanol for 6 hr. Completion of reaction was determined by using TLC. Later poured into hot water and then acidified with glacial acetic acid. The product was separated by filtration and recrystallize using glacial acetic acid (Figure 1).

Step-II

The mixture of compound 2, 4.58 g (20 mmol), methyl iodide, 5.68 g (40 mmol) and anhydrous potassium carbonate, 5.52 g (40 mmol) was stirred into DMF for 3 hr at room temperature. Reaction mixture was added into cold water and neutralized with glacial acetic acid. Residue recrystallizes with ethanol (Figure 2).

Step-III

The compound (3), 2.57 g (10 mmol) and hydrazine hydrate, 0.96 g (30 mmol) were heated in absolute ethanol for 6 hr. The reaction mixture was added into cold water and neutralized with glacial acetic acid. The solid was separated and recrystallized from suitable solvent (Figure 3).

Step-IV Synthesis of Compound (5a-5r)

The substituted intermediates were synthesized by the treatment of compound 4 (0.01 mol) with substituted aromatic aldehyde under reflux in ethanol for 5-6 hr. Later poured into ice cold water and solid residue recrystallized using ethanol (Figure 4).

Step-V

Synthesis of Compound (6a-r): The compounds (5a-r) (0.002 mol) and TEA (0.004 mol) was dissolved into 4-dioxane (50 mL), cooled and stirred for 15 to 20 min. To this solution chloroacetylchloride (0.004 mol) added drop wise within 20 min. Resultant solution was stirred for 3 hr and then refluxed for 8 hr. The final mixture was concentrated and poured into ice cold water and solid was separated by suction and recrystallized with glacial acetic acid (Figure 5).¹²

Fourier Transforms Infrared (FTIR) spectroscopy

The structure of compounds 5c-5r and 6c-6r were characterised by FTIR spectrophotometer at 4000 to 650 cm⁻¹.¹³

Nuclear Magnetic Resonance spectroscopy (NMR)

The NMR spectrum of all synthesized compounds (6c-6r) were recorded on (Bruker DRX 600 MHz) equipped with a TXI probe.¹⁴

In vitro Anticancer Activity

SRB assay

A cytotoxicity study was carried out to determine the anticancer potential of synthesized compound against colon HT29 and lung A549 cancer cell lines. Different concentrations (10, 20, 40 and 80 µg/mL) of synthesized compound (6c-6r) were used to treat the cells. A micro plate reader has been used to measure the absorption at 570 nm. The results were measured as GI₅₀ and LC₅₀.¹⁵

Morphological Evaluation of Apoptotic Cells

To measure the absorption of synthesized compounds by A549 and HT29 cells were sown on 24 well plates at a density of 5×10^4 cells per well and grown in 1 mL of growth media. The connected cells were given equal dosages of synthetic Compounds (6C-R) after 24 hr of incubation at 37°C and they were then maintained at that temperature in a 5% CO_2 incubator. The cells were given 1, 3 and 6 hr of incubation before being rinsed three times with buffer as well as lazed with methanol.¹⁶

Apoptosis by Flow Cytometer

Annexin V labelled with a fluorophore or biotin can identify apoptotic cells by binding to phospholipid exposed on the outer leaflet. Propidium Iodide (PI) is a fluorescent nucleus dye, impermeant to live cells and apoptotic cells, but stains dead cells with red fluorescence, binding tightly to the nucleic acids in the cell.¹⁷

Apoptosis by DAPI

A 24-well plate was used for the study which were kept at 37°C overnight in a CO_2 incubator. After treating the cells with formulations ($<50 \mu\text{g/mL}$), the cells have been kept for 24 hr incubation in a CO_2 incubator. PBS was used to wash the cells for about 30 min along with $20 \mu\text{L}$ of 4',6-Diamidino-2-Phenylindole (DAPI) staining solution ($0.1 \mu\text{g/mL}$) and further incubation in the dark. % of cells that have undergone apoptosis was calculated by randomly counting and selecting the apoptotic cells under microscopic fields.¹⁸

RESULTS

In silico studies

Compound 6C-R went to molecular docking investigation utilizing C-Docker software in Discovery Studio 2019. The precise intermolecular interactions between the ligands and proteins were examined using the C-DOCKER algorithm. The entry code PDB ID 2A4L from the PDB Databank was used to retrieve the 3D structural information for the targeted protein. The active site of the target protein was docked with the inhibitors and binding energies were assessed. This demonstrated that compounds with docking scores of 6R, 6L and 6P have higher scores than those with scores in the series. Compound 6R showed four Pi-alkyl bonds with LEU134, ILE10, VAL18 and ALA144 (4.47, 4.46, 5.29 and 5.04, respectively), one carbon-hydrogen bond with LEU83 (2.73), one Pi-donor hydrogen bond contact with GLU12 (3.18) and one H-bonding interaction with LYS89 (1.80) and one Pianion interaction with Asp145 (4.00), as shown in Figure 6. According to Figure 6, compound 6L had five H-bonding interactions with ASP86, GLU12, LYS89, HIS84 and LEU83 (2.04, 2.03, 1.81, 3.08 and correspondingly), two pi-alkyl interactions with ILE10 and LEU134 (5.0 and 4.66) and 2 carbon-hydrogen bonds with GLY13 and GLY11 (2.75 and 2.40). As seen in Figure 6, compound 6P interacted with four different molecules via hydrogen bonds: THR14, LYS33, ILE10 and LEU83 (2.63, 1.86, 2.79 and 2.31, respectively); three different molecules via pi-alkyl interactions: ALA31, VAL18 and LEU134 (5.19, 4.75 and 4.94, respectively); and four molecules via carbon-hydrogen bonds: GLY13, ASP145, PHE82 and LYS. The CDOCKER scores and chemical binding energies are displayed in Table 1.

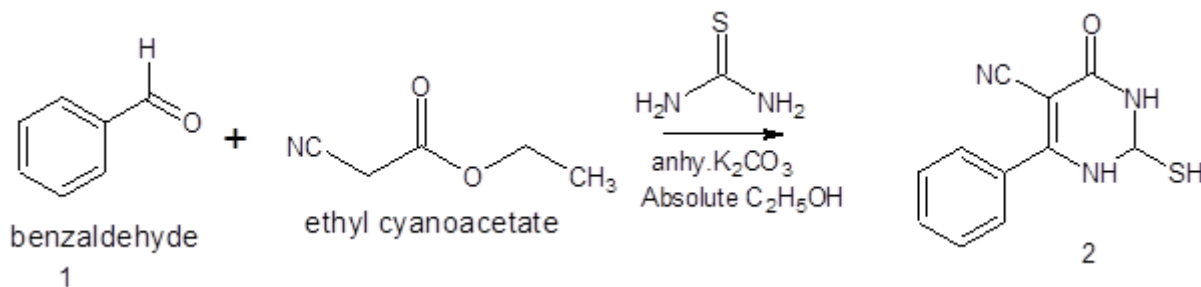


Figure 1: Synthesis of compound 2.

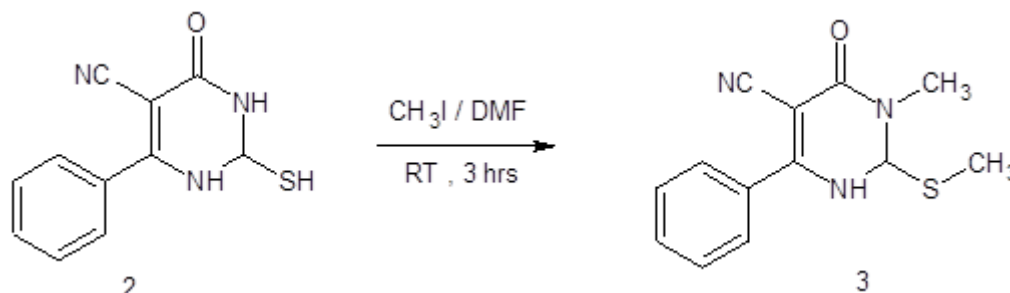


Figure 2: Synthesis of compound 3.

Chemistry

FTIR Interpretation

Structural elucidation of newly synthesized compounds was characterized by FTIR techniques for Compound (6C-R) described in Table 2 and Figure 7.

Nuclear Magnetic Resonance (NMR)

Structural elucidation of newly synthesized compounds was characterized by NMR technique and the resulting spectra are given in Table 3 and Figure 8.

The functional moieties present and the structures of newly synthesized compounds were characterized by the FT-IR and ¹H-NMR technique. We observed peaks for different functional groups of FT-IR (Å) at 1672 (C=O str), 2224 (CN), 1492 (C=C) and 887 (C-Cl) and NMR (Å) 8.74 (s, 1H, Ar-H), 7.24 (d, 2H, Ar H), 7.68 (d, 2H, Ar-H), 7.12 (d, 1H, Ar-H), 7.14 (s, 1H, NH). We observed OH functional group peaks for the molecule 6c, 6e, 6l, 6m for IR (Å) at 3312-3313 (str) and for NMR (ppm) at 6.8-7.0 (s, 1H, Ar-OH). OCH₃ group for the molecule 6c, 6l, 6p at 2860-2800 (str) and NMR at 3.8 (s, 3H, OCH₃); Br group for the molecule 6e, 6n for IR at 686-690 (str); NO₂ group for the molecule 6g, IR at 1400-1500 (str); N(CH₃)₂ group for the molecule at 3435 (str) and NMR at 3.11-3.15 (s, 3H, CH₃). Cl group for the molecule 6e at 858-887 (str). NH-N group for the molecule 6r at 1600 (str) and NMR at 2.10 (s, 1H, NH).

2-((3-chloro-2-(4-hydroxy-3-methoxyphenyl)-4-oxocyclobutyl)amino)-1-methyl-6-oxo-4-phenyl-1,6-dihydropyrimidine-5-carbonitrile(6c)

The molecular formula C₂₂H₁₈ClN₅O₄ and molecular weight was 451.87 gm/mol, R_f value: 0.61, melting point: 181-182°C. Elemental analysis (cal.): C, 58.48%; H, 4.02%; Cl, 7.85%; N, 15.50%; O, 14.16%; IR (KBR, cm⁻¹); 3212.96 (N-H str.), 1672.66 (C=O of β-lactum), 1601.43 (C=O stretch), 2224.15 (CN stretch), 1492.88 (C-H bend), 687.18 (C-Cl bending), ¹H-NMR (400 MHz, DMSO- d₆) δ 9.96 (s, 1H Ar-OH), 9.73 (s, 1H NH), 7.73 (d, 2H Ar-H), 7.69 (d, 2H Ar-H), 7.48 (s, 1H Ar-H), 7.38 (s, 1H Ar-H), 5.42 (s, 1H Benzylic-CH), 5.72 (s, 1H CH-CL of Azetidinone), 3.76 (s, 3H OCH₃), 3.52 (s, 3H, N-CH₃); m/z: 451.10, 453.10 (m+1), 452.10 (m+2).

2-((2-(3-bromo-5-chloro-2-hydroxy-3-chloro-4-oxocyclobutyl) amino)-1-methyl-6-oxo-4-phenyl-1,6-dihydropyrimidine-5-carbonitrile(6e)

The molecular formula of compound was C₂₁H₁₄BrCl₂N₅O₃ and molecular weight was 535.18 gm/mol, R_f value: 0.62, melting point: 198-200°C. Elemental analysis (cal.): C, 47.13; H, 2.64; Br, 14.93; Cl, 13.25; N, 13.25; O, 8.97; FT-IR (KBR, cm⁻¹) v_{max}: 3306.82(NH stretch), 3082.29 (Ar CH stretch), 2924.56 (CH stretch), 2214.73 (C=N stretch), 1675.07 (C=O stretch), 1581.59 (C=C stretch), 736 (C-Br stretch), 690.90 (C-Cl stretch), 618, 675.35, 748.34, 788.42 (aromatic region). ¹H NMR; 10.56 (s, 1H, NH), 10.01 (s, 1H OH), 8.56 (d, 2H), 7.74 (s, 1H), 7.52 (m, 4H), 7.23 (s, 1H), 5.08 (s, 1H benzylic-CH), 5.55 (s, 1H, azetidinone

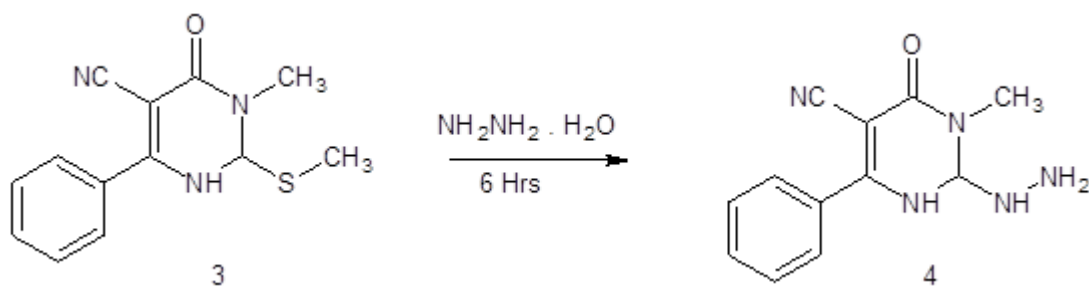


Figure 3: Synthesis of compound 4.

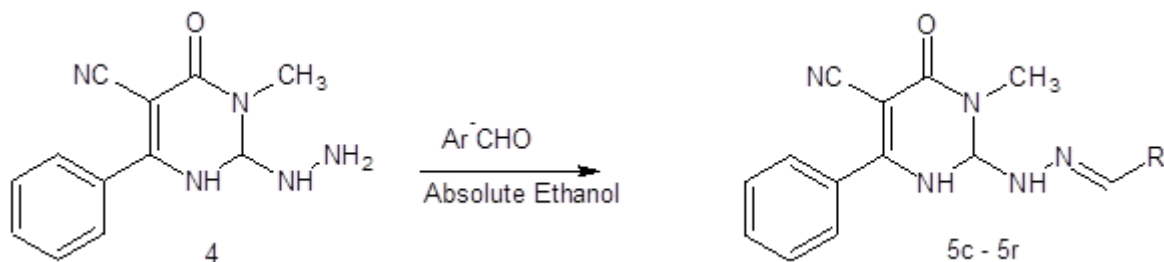


Figure 4: Synthesis of compound 5c-5r.

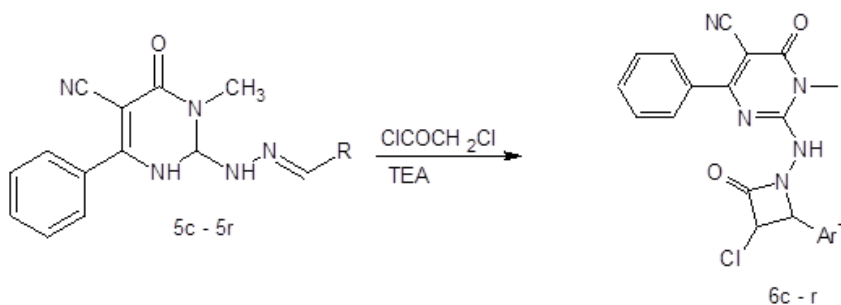


Figure 5: Synthesis of compound 6c-6r.

Table 1: CDOCKER Scores and Binding Energy of Pyrimidine Derivatives (6c-6r).

Compounds	Binding Energy	-CDOCKER Energy	-CDOCKER Interaction Energy
6c	-71.3769	9.87398	62.8858
6e	-82.6398	10.6211	55.1391
6f	-81.8044	17.7161	58.578
6g	-85.1675	-0.6733	58.4209
6l	-145.309	22.732	64.6716
6m	-87.777	1.37079	61.1818
6n	-80.4302	20.0373	63.134
6o	-131.973	8.00179	61.7941
6p	-59.5702	9.01891	64.4786
6r	-82.7588	-16.2075	55.9064

CH-Cl), 3.41 (s, 3H, N-CH₃); *m/z*; 532.97, 533.97, 534.96, 535.96, 536.96, 537.97, 538.96.

2-((3-chloro-2-(4-dimethylamino phenyl)-4-oxocyclobutyl) amino)-1-methyl-6-oxo-4-phenyl-1,6-dihydropyrimidine-5-carbonitrile(6f)

The molecular formula C₂₃H₂₁ClN₆O₂ and molecular weight of 448.51 gm/mol, R_f value:

0.62, melting point: 202-204°C. Elemental analysis (cal.): C, 61.54; H, 4.72; Cl, 7.90; N, 18.72; O, 7.13; FT-IR (KBR, cm⁻¹) v_{max}: 3435.19(NH stretch), 3339.68(CH stretch), 2912.54 (CH stretch), 2223.98 (C=N stretch), 1681.91 (C=O stretch), 1612.91 (C=C stretch), 691.20(C-Cl stretch), 617, 681.35, 751.88, 792.68 (aromatic region). 1H NMR; 10.39(s, 1H, NH), 8.32 (d, 2H), 7.89 (s, 1H), 7.74 (m, 4H), 7.50 (s, 1H), 5.05 (s, 1H benzylic-CH), 5.51 (s, 1H, azetidinone CH-Cl), 3.35 (s, 3H, N-CH₃), 3.00 (m 6H); *m/z*; 448.14, 449.14, 450.14, 451.14.

2-((3-chloro-2-(3-nitro phenyl))-4- oxocyclobutyl) amino)-1-methyl-6-oxo-4-phenyl-1,6dihydropyrimidine-5-carbonitrile(6g)

The molecular formula of the compound was C₂₁H₁₅ClN₆O₄ and molecular weight was 450.84 gm/mol, R_f value: 0.62, melting point: 212-214°C. Elemental analysis (cal.): C, 55.95; H, 3.35; Cl, 7.86; N, 18.64; O, 14.19; FT-IR (KBR, cm⁻¹) v_{max}: 3330.12 (NH

stretch), 3240.84 (CH stretch), 3062.26 (Ar CH stretch), 2935.14 (CH stretch, Azetidinone), 2223.99 (CN stretch), 1669.93 (C=O stretch), 1599.13 (C=C stretch), 1490.03 (NO stretch), 1352.04 (C-N stretch), 1570.51 (N-H Stretch), 1626.50 (C=C stretch), 1745.60 (C-H bend), 1696.59 (C=N Stretch), 687.61 (C-Cl stretch), 617, 681.35, 751.88, 792.68 (aromatic region). 1H NMR; 9.97 (s, 1H, NH), 8.61 (d, 2H), 8.22 (s, 1H), 7.76 (m, 4H), 7.54 (s, 1H), 5.09 (s, 1H benzylic-CH), 5.29 (s, 1H, azetidinone CH-Cl), 3.40 s, 3H, N-CH₃); *m/z*; 450.08, 452.08, 451.09, 453.08.

2-((3-chloro-2-(3,4,5-trihydroxyphenyl) cyclobutyl)amino)-1-methyl-6-oxo-4-phenyl-1,6dihydropyrimidine-5-carbonitrile.(6l)

The molecular formula of the 6l was C₂₁H₁₆ClN₅O₅ and molecular weight was 453.84 gm/mol, R_f value: 0.62, melting point: 128-131°C. Elemental analysis (cal.): C, 55.58; H, 3.55; Cl, 7.81; N, 15.43; O, 17.63; FT-IR (KBR, cm⁻¹) v_{max}: 3618.76 (OH stretch), 3313.98 (NH stretch), 3248.32 (CH stretch), 3058.12 (Ar CH stretch), 2933.57 (CH stretch, Azetidinone), 2219.25 (CN stretch), 1669.30 (C=O stretch), 1605.37 (C=C stretch), 1376.88(C-N stretch), 1572.32 (N-H Stretch), 686.32 (C-Cl stretch), 622, 669, 748, 791 (aromatic region). 1H NMR; 9.97 (s, 1H, NH), 8.61 (d, 2H), 8.22 (s, 1H), 7.76 (m, 4H), 7.54 (s, 1H), 5.09 (s, 1H benzylic-CH), 5.29 (s, 1H, azetidinone CH-Cl), 3.40 (s, 3H, N-CH₃); *m/z*; 450.08, 452.08, 451.09, 453.08.

2-((3-chloro-2-(2-hydroxyphenyl)-4-oxocyclobutyl)amino)-1-methyl-6-oxo-4-phenyl-1,6-dihydropyrimidine-5-carbonitrile.(6m)

The molecular formula of the compound was $C_{21}H_{16}ClN_5O_3$, and molecular weight: 421.84 gm/mol, R_f value: 0.62, melting point: 184-186°C. Elemental analysis (cal.): C, 59.79; H, 3.82; Cl, 8.40; N, 16.60; O, 11.38; FT-IR (KBR, cm^{-1}) ν_{max} : 3621.32 (OH stretch), 3308.28 (NH stretch), 3272.17 (CH stretch), 3056.38 (Ar CH stretch), 2921.62 (CH stretch, Azetidinone), 2217.20 (CN stretch), 1670.14 (C=O stretch), 1606.65 (C=C stretch), 1425.33, 1376.88 (C-N stretch), 1546.07 (N-H Stretch), 694.46 (C-Cl stretch), 621, 672, 748, 792 (aromatic region). 1H NMR; 10.32 (s, 1H, NH), 8.68 (d, 2H), 7.89 (s, 1H), 7.76 (m, 4H), 7.74 (s, 1H), 5.00 (s, 1H benzylic-CH), 5.45 (s, 1H, azetidinone CH-Cl), 3.40 (s, 3H, N-CH₃); m/z; 424.09, 421.09, 423.09, 422.10, 453.08.

2-((3-chloro-2-(3,5-dibromophenyl)-4-oxocyclobutyl)amino)-1-methyl-6-oxo-4-phenyl-1,6-dihydropyrimidine-5-carbonitrile.(6n)

The molecular weight was 563.63 gm/mol, R_f value: 0.62, melting point: 196-198°C.

Elemental analysis (cal.): C, 44.83; Br, 28.40%, H, 2.33; Cl, .30; N, 12.45; O, 5.69; FT-IR (KBR, cm^{-1}) ν_{max} : 3326.66(NH stretch), 3274.28 (CH stretch), 3074.44 (Ar CH stretch), 2926.33 (CH stretch, Azetidinone), 2219.66 (CN stretch), 1681.64 (C=O stretch), 1621.43 (C=C stretch), 1426.58, 1227.80 (C-N stretch), 1537.81 (N-H Stretch), 853.75 (C-Br stretch), 683.90 (C-Cl stretch), 626, 668, 752, 789 (aromatic region). 1H NMR; 9.96 (s, 1H, NH), 8.18 (s, 2H), 7.81 (s, 1H), 7.76 (m, 3H), 7.58 (d, 2H), 5.01 (s, 1H benzylic-CH), 5.54 (s, 1H, azetidinone CH-Cl), 3.41 (s, 3H, N-CH₃); m/z; 561.91, 559.91, 562.91, 563.91, 564.91, 565.91.

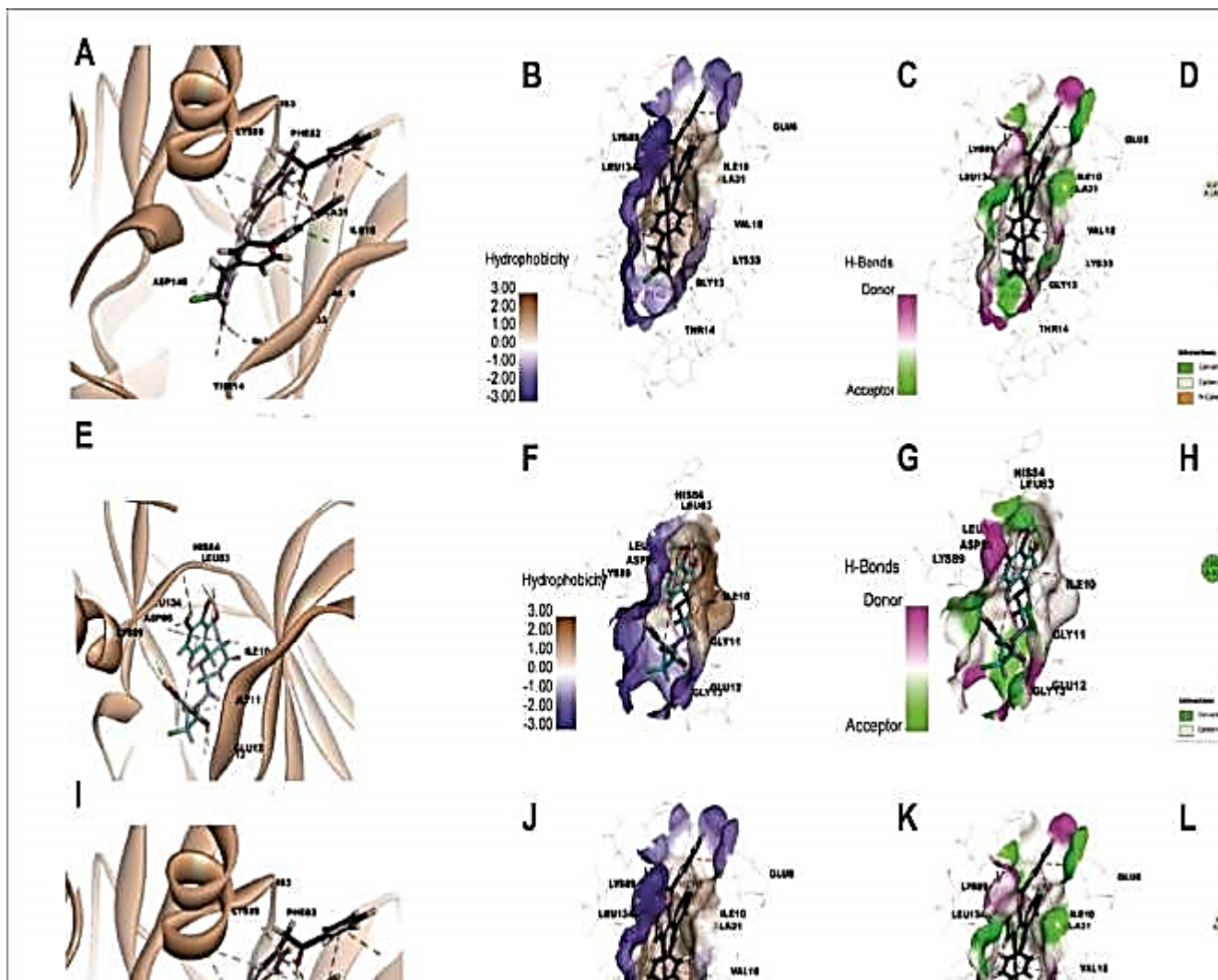


Figure 6: 3D Interaction of compound 6r at the binding site of the enzyme (PDB ID: 2A4L). (A) Interaction with Protein 2A4L, (B) Hydrophobic interaction, (C) Hydrogen bond interaction, (D) 2D Interaction of the compound 6r at the active site of the enzyme 2A4L; 3D Interaction of compound 6l at the binding site of the enzyme (PDB ID: 2A4L) (E) Interaction with Protein 2A4L, (F) Hydrophobic interaction, (G) Hydrogen bond interaction, (H) 2D Interaction of the compound 6r at the active site of the enzyme 2A4L; 3D Interaction of compound 6p at the binding site of the enzyme (PDB ID: 2A4L) (I) Interaction with Protein 2A4L, (J) Hydrophobic interaction, (K) Hydrogen bond interaction, (L) 2D Interaction of the compound 6r at the active site of the enzyme 2A4L.

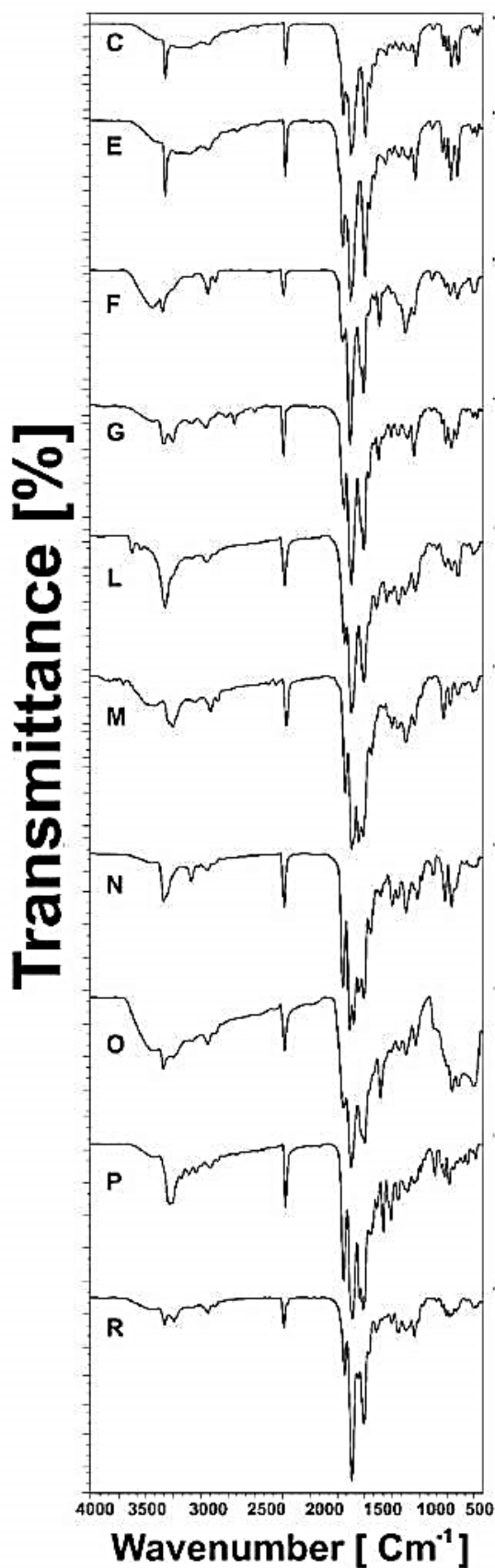


Figure 7: FTIR Interpretation Data of Pyrimidine Derivatives (6C-R).

2-((3-chloro-2-(4-morpholinophenyl)-4-oxocyclobutyl)amino)-1-methyl-6-oxo-4-phenyl-1,6-dihydropyrimidine-5-carbonitrile.(6o)

The molecular formula $C_{25}H_{23}ClN_6O_3$ and molecular weight was 490.95 gm/mol, R_f value:

0.62, melting point: 198-200°C. Elemental analysis (cal.): C, 61.16; H, 4.72; Cl, 7.22; N, 17.12; O, 9.78; FT-IR (KBR, cm^{-1}) ν_{max} : 3333.97(NH stretch), 3243.27 (CH stretch), 2924.39 (CH stretch morpholine), 2857.76 (CH stretch morpholine), 2220.91 (C=N stretch), 1610.31 (C=O stretch), 1486.52(C=C stretch), 1340.68 (C=C stretch), 1169.01 (C-O-C stretch), 682.43 (C-Cl stretch) 619, 682.12, 749.21, 791.39 (aromatic region). NMR; 9.96 (s, 1H), 8.02-7.75 (d, 2H), 7.50-7.74 (m, 4H), 7.49-7.47 (m, 4H), 5.48 (s, 1H), 5.02 (s, 1H), 3.69 (d, 2H), 3.41 (m, 5H), 3.36 (t, 3H); m/z; 490.15, 491.16, 492.15, 493.15.

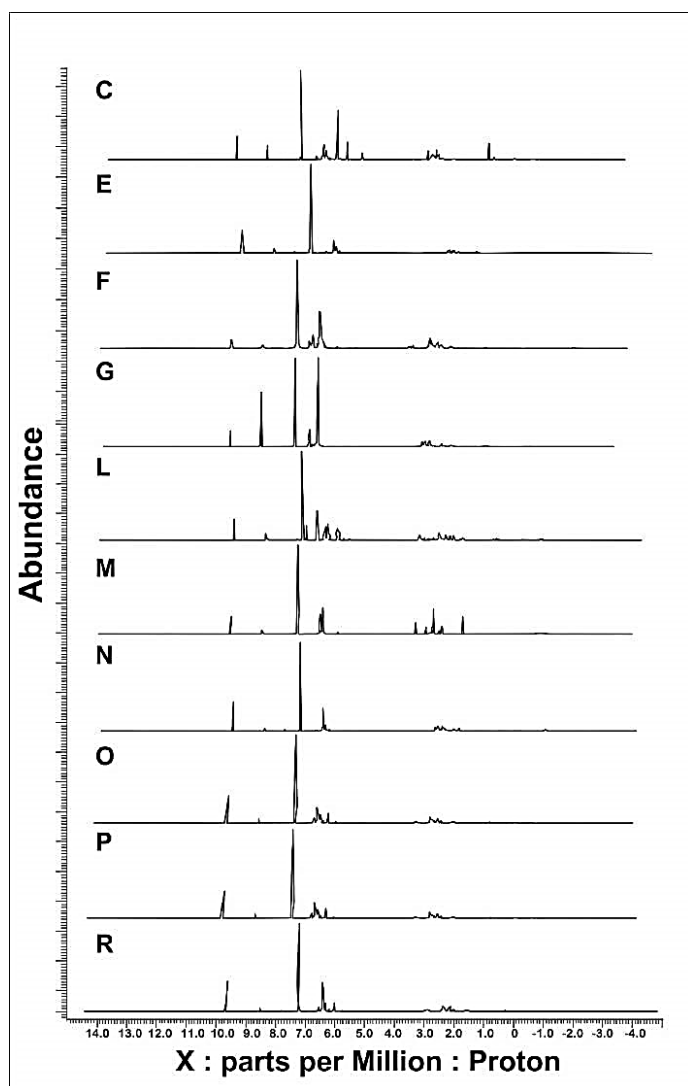


Figure 8: NMR Interpretation Data of Pyrimidine Derivatives (6C-R).

N-(4-((2-chloro-4-((5-cyano-1-methyl-6-oxo-4-phenyl-1,6-dihydropyrimidine-2yl)amino)-3-oxocyclobutyl)phenylacetamide.(6p)

The molecular formula $C_{23}H_{19}ClN_6O_3$ and molecular weight was 462.89 gm/mol, R_f value: 0.62, melting point: 221-223°C. Elemental analysis (cal.): C, 65.15; H, 4.59; Cl, 7.69; N, 12.16; O, 10.41; FT-IR (KBR, cm^{-1}) ν_{max} : 3285.66 (NH stretch), 2221.84 (C=N stretch), 1681.57 (C=O stretch, Azetidinone), 1599.50 (C=O stretch), 1537.32 (C=C stretch), 1501.08 (Ar C=C stretch), 1435.68 (Ar C=C stretch), 1373.14 (CN stretch), 1175.36 (CO stretch), 695.28 (C-Cl stretch), 615, 689.12, 740.85 (aromatic region). 1H NMR: 10.14 (s, 1H), 9.81 (s, 1H), 8.41-7.41 (m, 9H), 5.47 (s, 1H), 5.08 (s, 1H), 3.26 (t, 3H), 2.02 (s, 3H), m/z; 460.13, 462.13, 461.13.

2-((2-(3-bromo-4-hydroxy-5-methoxyphenyl)-3-chloro-4-oxocyclobutyl)amino)-1-methyl-6-oxo-4-phenyl-1,6-dihydropyrimidine-5-carbonitrile(6r)

The molecular formula and $C_{22}H_{17}BrClN_5O_4$, molecular weight was 530.76 gm/mol, R_f value: 0.64, melting point: 192-194°C. Elemental analysis (cal.): C, 49.79; H, 3.23; Cl, 6.68; N, 13.20; O, 12.06; FT-IR (KBR, cm^{-1}) ν_{max} : 3317.09 (NH stretch), 3233.19 (CH stretch), 2922.37(CH stretch), 2855.58 (CH stretch), 2223.69 (C=N stretch), 1668.06 (C=O stretch, Azetidinone), 1599.07 (C=O stretch), 1490.94 (C=C stretch), 1444.69 (C=C stretch), 1376.92 (CN stretch), 1134.37 (OCH₃ Strech), 869.24 (C-Br stretch), 734.14 752, 793, 734 (C-Cl stretch), 683 (aromatic region). 1H NMR: 9.69 (s, 2H), 8.36(s, 1H), 8.34 (d, 2H), 7.71 (s, 1H), 6.96 (s, 1H), 5.57 (s, 1H), 5.03 (s, 1H), 3.69 (t, 3H), 3.38 (t, 3H); m/z; 529.02, 531.01, 533.01, 530.02, 534.01.

Table 2: FTIR Interpretation Data of Pyrimidine Derivatives (6c-6r).

Compound	Molecular Formula	Mol. Wt.	M.P.	FTIR Interpretation Data
6c	$C_{22}H_{18}ClN_5O_4$	451.86	236-238	3312 (OH str), 1672 (C=O str), 2224 (CN), 1492 (C=C) and 887 (C-Cl).
6e	$C_{21}H_{14}BrCl_2N_5O_3$	535.18	268-270	3306 (OH str), 1675 (C=O str), 2214 (CN), 1496 (C=C), 738 (C-Cl) and 690 (C-Br).
6f	$C_{23}H_{21}ClN_6O_2$	448.90	256-258	3435 (N-(CH ₃) ₂), 1612 (C=O str), 2223 (CN), 1490 (C=C) and 858 (C-Cl).
6g	$C_{21}H_{15}ClN_6O_4$	450.83	246-248	3330 (NH str), 1669 (C=O str), 2223 (CN), 1443 (C=C), 1352 (NO ₂) and 865 (C-Cl).
6l	$C_{22}H_{17}BrClN_5O_4$	530.76	266-268	3313 (OH str), 1605 (C=O str), 2219 (CN), 1491 (C=C), 741 (C-Cl) and 686 (C-Br).
6m	$C_{21}H_{16}ClN_5O_3$	421.83	252-254	3308 (OH str), 1606 (C=O str), 2217 (CN), 1505 (C=C) and 753 (C-Cl).
6n	$C_{21}H_{14}Br_2ClN_5O_2$	563.62	266-268	3306 (OH str), 1621 (C=O str), 2219 (CN), 1426 (C=C), 853 (C-Cl) and 744 (C-Br).
6o	$C_{25}H_{23}ClN_6O_3$	490.94	280-282	3333 (NH str), 1610 (C=O str), 2220 (CN), 1482 (C=C), 1104 (C-O-C) and 682 (C-Cl).
6p	$C_{23}H_{19}ClN_6O_3$	462.89	246-248	3285 (NH str), 1599 (C=O str), 2221 (CN), 1435 (C=C), 1104 (C=O Ketone) and 832 (C-Cl).
6r	$C_{29}H_{23}ClN_6O_3$	538.98	234-236	3317 (NH str), 1599 (C=O str), 2223 (CN), 1490 (C=C), 1668 (C=O Ketone) and 734 (C-Cl).

Anticancer activity

Cytotoxicity

In vitro anticancer effects of newly synthesized Compounds (6C-R) on colon (HT-29) and lung (A549) cancer cells by SRB assay. Synthesized compounds were dissolved in DMSO and each drug was examined at different concentrations (10, 20, 40 and 80 µg/mL). In each experiment, an appropriate positive control (reference) drug Adriamycin (ADR) was employed. The results are described in Table 4 in terms of GI_{50} , TGI and LC_{50} . The data showed that the 50% Inhibitory concentration values (GI_{50}) have moderate to good activity using ADR as a reference molecule on colon and lung cancer, with values ranging from

1.2 to 17.2 µg/mL and 1.2 to 17.2 µg/mL, respectively. The drug concentration that results in Total Inhibition of cells (TGI) for lung cancer by compounds 6L and 6M, respectively, is 10.0 µg/mL and 17.2 µg/mL for colon cancer, exhibiting better potency. The remaining compounds showed moderate action, however 6G and 6L showed no activity. Maximum inhibitory action for the four dose levels of compounds was discovered at 80 µg/mL. The percentage control growth results of Compound (6C-R) on colon (HT-29) and lung (A549) cancer cell lines, respectively, are shown in Table 4 with reference to ADR. Thus it is confirmed that the compound 6L=2-[[3-chloro-2-oxo-4-(3,4,5trihydroxyphenyl) azetid in-1-yl] amino]-1-methyl-6-oxo-4-phenyl-

Table 3: NMR Interpretation Data of Pyrimidine Derivatives (6c-6r).

Compound	Molecular Formula	Mol. Wt.	M.P.	NMR Interpretation Data
6c	$C_{22}H_{18}ClN_5O_4$	451.86	236-238	8.74 (s, 1H, Ar-H), 7.24 (d, 2H, Ar H), 7.68 (d, 2H, Ar-H), 7.12 (d, 1H, Ar-H), 7.14 (s, 1H, NH).
6e	$C_{21}H_{15}Br_2ClN_6O_2$	578.64	268-270	8.63 (s, 1H, Ar-H), 7.31 (d, 2H, Ar H), 7.34 (d, 2H, Ar-H), 7.06 (d, 1H, Ar-H), 7.10 (s, 1H, NH).
6f	$C_{21}H_{14}Br_2ClN_5O_3$	579.62	256-258	8.45 (s, 1H, Ar-H), 7.12 (d, 2H, Ar H), 7.42 (d, 2H, Ar-H), 7.11 (d, 1H, Ar-H), 7.18 (s, 1H, NH), 2.21 (s CH3).
6g	$C_{21}H_{14}BrClN_6O_4$	529.73	246-248	8.23 (s, 1H, Ar-H), 7.65 (d, 2H, Ar H), 7.08 (d, 2H, Ar-H), 7.12 (d, 1H, Ar-H), 7.04 (s, 1H, NH).
6l	$C_{21}H_{16}ClN_5O_5$	453.83	266-268	8.22 (s, 1H, Ar-H), 7.28 (d, 2H, Ar H), 7.45 (d, 2H, Ar-H), 7.12 (d, 1H, Ar-H), 7.08 (s, 1H, NH).
6m	$C_{22}H_{18}ClN_5O_4$	451.86	252-254	δ 7.88, δ 7.72 and δ 7.69 (Ar-H), δ 2.78 (NH-N), δ 3.11 (N-CH3), 8.22 (s, 1H, Ar-H), 7.43 (d, 1H, Ar-H), 7.04 (d, 1H, Ar-H), 11.96 (s, 1H, NH).
6n	$C_{21}H_{14}Cl_2IN_5O_2$	566.17	266-268	δ 7.58, δ 7.68 and δ 7.88 (Ar-H), δ 2.34 (NH-N), δ 3.15 (N-CH3), δ 5.74 (C-Cl), 8.10 (s, 1H, Ar-H), 7.14 (d, 1H, Ar-H), 7.26 (d, 1H, Ar-H), 11.92 (s, 1H, NH).
6o	$C_{25}H_{23}ClN_6O_3$	490.94	280-282	δ 7.74, δ 7.68 and δ 7.91 (Ar-H), δ 2.10 (NH-N), δ 3.12 (N-CH3), 8.10 (s, 1H, Ar-H), 7.14 (d, 1H, Ar-H), 7.26 (d, 1H, Ar-H), 11.92 (s, 1H, NH).
6p	$C_{28}H_{21}ClN_6O_3$	524.95	246-248	δ 7.88, δ 7.72 and δ 7.68 (Ar-H), δ 2.08 (NH-N), δ 3.11 (N-CH3), 8.14 (s, 1H, Ar-H), 7.11 (d, 1H, Ar-H), 7.21 (d, 1H, Ar-H), 11.96 (s, 1H, NH).
6r	$C_{28}H_{23}ClN_6O_2$	510.97	234-236	δ 7.91, δ 7.88 and δ 7.64 (Ar-H), δ 2.02 (NH-N), δ 3.08 (N-CH3), δ 4.44 (d 2H NHCH2) 8.11 (s, 1H, Ar-H), 7.02 (d, 1H, Ar-H), 7.14 (d, 1H, Ar-H), 11.76 (s, 1H, NH).

Table 4: Anticancer activity of Pyrimidine Derivatives (6c-6r) on HT-29 and A549 Cell lines.

Sample Codes	HT-29						A549					
	LC ₅₀	SD	TGI	SD	GI ₅₀ *	SD	LC ₅₀	SD	TGI	SD	GI ₅₀ *	SD
6- (c)	64.2	3.6	36.8	2.3	9.4	1.7	>80	14.65	56.8	9.32	31.9	7.07
6- (e)	78.5	3.5	54.5	2.8	30.5	1.2	60.9	5.3	33.8	3.8	6.7	2.2
6- (f)	>80		49.1	4.5	12.0	1.9	>80		64.6	6.9	41.7	5.4
6- (g)	NE		>80		66.4	12.4	NE	-	>80		>80	23.4
6- (l)	61.5	2.8	15.0	1.9	<10	0.5	76.5	12.54	55.8	7.2	35.1	5.7
6- (m)	66.1	0.7	10.0	1.1	<10	0.7	>80		36.1	2.4	<10	0.77
6- (n)	>80		92.6	3.2	22.18102	2.4	>80		>80		50.61836	8.46
6- (o)	66.2	0.4	36.8	1.2	7.4	0.4	>80		57.2	5.9	30.3	4.45
6- (p)	66.6	0.9	42.0	1.7	17.3	0.9	78.4	6.5	55.7	5.2	33.0	4.3
6- (r)	NE		NE		>80		NE	-	NE	-	>80	4.9
ADR	NE		NE		<10	0.4	NE	-	<10	1.5	<10	0.7

LC₅₀-Concentration of drug causing 50% cell kill.

GI₅₀-Concentration of drug causing 50% inhibition of cell growth.

TGI-Concentration of drug causing total inhibition of cell growth.

GI₅₀-Values of <10 µg is considered to demonstrate potent activity in of pure case compounds and NE-No effect.

1,6-dihydropyrimidine-5-carbonitrile and 6M=2-[[3-chloro-2-(3-hydroxy-4-methoxyphenyl)-4-oxoazetidin-1yl]amino]-1-methyl-6-oxo-4-phenyl-1,6-dihydropyrimidine-5-carbonitrile has strong anticancer potential in treatment of colon and lung cancer respectively and used as lead molecules for further processes.

Morphological evaluation of apoptotic cells

Cell morphology was used to study the anticancer potential of synthesized compounds 6L and 6M by evaluating morphological changes. Figure 9 depicts A549 cells treated with 6L compound and HT29 cells treated with 6M for 48 hr. For lung cancer in the control group, the cells observed were spindle-shaped and showed higher confluence of monolayer cells (Figure 9A). In contrast, A549 cells treated with 6L (Figure 9C), lost their normal morphology, shrank, detached and showed a more significant reduction in the number. For colon cancer in the control group, the cells observed were somewhat oval-shaped and showed higher confluence of monolayer cells (Figure 9E). In contrast, HT29 cells treated with 6M (Figure 9G), lost their normal morphology, shrank, detached and showed a more significant reduction in the number.^{19,20}

Apoptosis by Flowcytometer

To examine whether synthesized compounds induce cell death in tumours tissues, the apoptosis-inducing potential of 6L and 6M in A549 and HT29 cells was determined by the annexin-V FITC/PI staining technique. In the case of lung cancer, the untreated cells were mostly healthy, with 98.30% of live cells, 0.14% of apoptosis and 1.26% of necrotic cell states, as shown in Figure 10A. When treated with 6L, the percentage of live cells decreased from 98.30% to 73.70% (Figure 10B). 6L-treated cells showed that 3.58% of the cells were apoptotic and 22.7% of the cells were necrotic. Untreated colon cancer cells, on the other hand, were mostly healthy, with 99.2% of live cells, 0.01% of apoptosis and 0.73% of necrotic cell states, as shown in Figure 10C. When treated with 6m, the percentage of live cells decreased from 99.2% to 83.48% (Figure 10D). 6M-treated cells showed that 3.11% of the cells were apoptotic and 13.5% of the cells were necrotic. Both 6M and 6L exhibit significant ($p < 0.05$) induction of apoptosis when compared to untreated cells. Similarly, in comparison to 6M and 6L, they showed significant ($p < 0.05$) induction of the apoptosis mode of death.^{21,22}

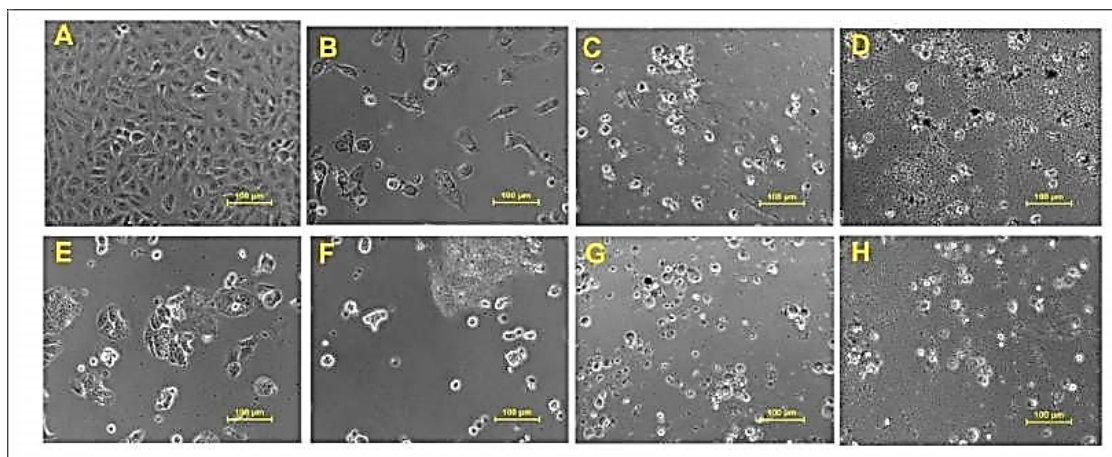


Figure 9: The morphological variations in HT29 cells A) Control B) ADR Treated C) 6L D) 6M, Morphological variations in A549 cells E) Control F) ADR Treated G) 6L H) 6M Treated cells for 48 hr.

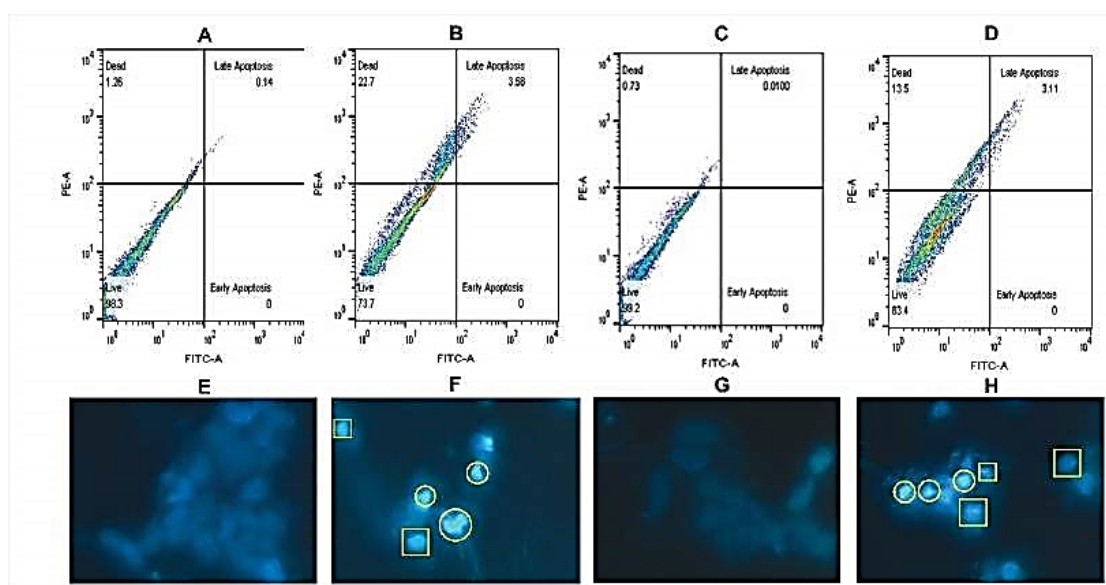


Figure 10: Flow cytometry A) Control HT29 cells B) 6L Treated C) Control A549 cells D) 6M Treated; DAPI Apoptosis E) Control HT29 cells F) 6L Treated G) Control A549 cells H) 6M Treated cancer cells after 24 hr of incubation. Circle represents chromatin condensation and nuclear shrinkage and square represents nuclear blebbing and nuclear fragmentation.

DAPI

The DAPI staining assay is a unique method used to determine alterations in nuclear morphology. In the case of lung (Figure 10E) and colon (Figure 10F) cancer, the untreated cells had weak, uniformly blue stained normal nuclei, whereas 6L (Figure 10G) and 6M (Figure 10H) treated lung and colon cancer cells, respectively, showed bright chromatin condensation, nuclear fragmentation and the appearance of small nuclei (apoptotic bodies). The induction of apoptosis in cells is confirmed by nuclear morphological changes.²³ These changes could be caused by cell permeability, activation of the enzyme responsible for apoptosis.²⁴ Identical findings have also been reported in the literature.^{25,26}

DISCUSSION

In present study, we have designed and developed some pyrimidine derivatives as potential cyclin dependent kinase inhibitors. The pyrimidine derivative was screened through molecular docking studies and subjected for synthesis followed by *in vitro* anticancer activity. The binding affinities of the derivatives have been compared with the binding mode of native ligand present in the crystal structure of cyclin dependent kinase enzyme (PDB ID: 2A4L). Native ligand (naquotinib) displayed -8.3 kcal/mol binding affinity with CDK-2 and formed three conventional and one carbon-hydrogen bond with Gly857, Glu762 and Glu758. It has developed electrostatic (Pi-anion, attractive charge) and hydrophobic bonds (alkyl and Pi-alkyl) with Glu758, Glu762, Ala755, Pro877 and Leu858. All the designed molecules displayed most potent interactions than the native ligand.

6c exhibited -9 kcal/mol docking score and formed four conventional and one carbon-hydrogen bond with Asp855, Arg841 and Lys745. Most interestingly it has formed one Pi-donor hydrogen bond (Pi-sulfur) with Cys797 which is mutated amino acid residue for the second generation CDK-2 inhibitors. It has developed many hydrophobic interactions with Val726, Arg841, Leu718, Ala743, Leu844 and Leu858. It has formed Pi-sulfur bond with Met790 which is mutated amino acid residue and developed resistance to the third generation EGFR inhibitors.

6l displayed -9.3 kcal/mol binding affinity and formed four potent conventional hydrogen bonds with Asp855, Lys745, Cys797 and Arg841. It has formed one Pi-donor hydrogen bond (Pi-sulfur) with Cys797. It exhibited one Pi-anion bond with Asp837. It has developed many hydrophobic interactions with Val726, Leu844, Met790, Arg841, Leu718, Ala743 and Leu858. 6p demonstrated -9.3 kcal/mol docking score and formed three conventional and one carbon-hydrogen bond with Asp855, Lys745 and Arg841. It has formed two electrostatic bonds with Asp837 and Asp855. It has also developed many hydrophobic interactions with the amino acids same as developed by 6c and 6p.

All the synthesized compounds induced the cytotoxicity to A549 and HT-29 and displayed good range of IC_{50} values in between 4 to 59 $\mu\text{m}/\text{mL}$. Against HT-29, out of all the tested compounds, 6m and 6n exerted good IC_{50} value i.e 4.98 and 9.66 $\mu\text{m}/\text{mL}$, respectively and compound 6c and 6p shows good IC_{50} value i.e 19.38 and 20.47 $\mu\text{m}/\text{mL}$ against A549 respectively. As compared to standard it exhibited significant cytotoxic effect on tested cell lines. The annexin V-FITC/PI staining differentiates cells into four clusters namely, live, early apoptosis, late apoptosis and necrotic cells. The untreated cells in the control sample were predominantly healthy (98.0% live cells) with only 0.0%, 0.16% and 1.11% of the cells were in early apoptotic, late apoptotic and necrotic states. The percentage of live cells decreased from 98.0% to 68.4% when treated with synthesized compound.

The apoptosis-inducing capability of synthesized derivatives was further confirmed using the annexin V-FITC/PI staining technique, which distinguished between necrosis and apoptosis. The significant proportion of cells in early and late apoptotic states following synthesized derivatives treatment highlights its effectiveness in inducing programmed cell death in cancer cells.^{27,28} Our results are in accord with previous published literature reported fragmentation of nuclei and uneven edges nearby the nuclei in cells treated with synthesis synthetic derivative can able to induce apoptosis in carcinogenic cells.^{29,30}

CONCLUSION

From the results, it is concluded that docking study demonstrated that compounds with docking scores of 6R, 6L and 6P have higher scores than those with scores in the series. Among all newly synthesized pyrimidine fused with azetidone derivatives (6C-6R)

derivatives, the most potent anticancer activity was displayed by 6L and 6M on HT-29 and A549 cell lines, respectively. It also significantly ($p < 0.001$) inhibited the proliferation and induces apoptosis significantly ($p < 0.001$) in colon (HT29) and lung (A549) cancer. Pyrimidine fused with azetidone derivatives (6C-6R) derivatives is a promising approach to design new anticancer moieties with strong anticancer potential. However, further *in vivo* animal studies are required to establish its efficacy in the treatment of cancer.

ACKNOWLEDGEMENT

The authors are Thankful to Department of Pharmacy, Vels University Chennai and Tamilnadu for providing required guidance and support for completion of present research work.

CONFLICT OF INTEREST

The authors declare that there is no conflict of interest.

ABBREVIATIONS

HT29: Colon cancer cell lines; **A549:** Lung cancer cell lines; **SRB:** Sulforhodamine B protein; **LC_{50} :** Concentration of drug causing 50% cell kill; **GI_{50} :** Concentration of drug causing 50% inhibition of cell growth; **TGI:** Concentration of drug causing total inhibition of cell growth; **FGI_{50} :** Values of $< 10 \mu\text{m}$ is considered to demonstrate potent activity in of pure case compounds and NE-No effect.

SUMMARY

In present study, we have designed and developed some azetidone-thiazole based pyrimidine derivatives as potential EGFR inhibitors. The designed derivative were screened through molecular docking studies and subjected for synthesis followed by *in vitro* anticancer activity. The binding affinities of the derivatives have been compared with the binding mode of native ligand present in the crystal structure of EGFR enzyme (PDB ID: 2A4l). All the designed molecules displayed most potent interactions than the native ligand. Most interestingly many molecules had formed one Pi-donor hydrogen bond (Pi-sulfur) or conventional hydrogen bond with Cys797 which is mutated amino acid residue for the second generation EGFR inhibitors. Many molecules had formed Pi-sulfur bond with Met790 which is mutated amino acid residue and developed resistance to the third generation EGFR inhibitors. All the interaction results presented here suggest this molecule has potential to be developed as most potent 4th generation EGFR inhibitors which will might have effectiveness against triple mutant T790M/C797S EGFR. From this investigation, it was decided to synthesize all the designed molecules with their biological evaluation. *In vitro* cytotoxicity of synthesized compounds against HT-29 (Colon Cancer) and A549 (lung cancer) were carried out using SRB assay.

REFERENCES

- Morgan E, Arnold M, Gini A, Lorenzoni V, Cabasag CJ, Laversanne M, et al. Global burden of colorectal cancer in 2020 and 2040: incidence and mortality estimates from GLOBOCAN. *Gut*. 2023; 72(2): 338-44. doi:10.1136/gutjnl2022-327736, PMID 36604116.
- Peram MR, Jalalpure S, Kumbhar V, Patil S, Joshi S, Bhat K, et al., Factorial design based curcumin ethosomal nanocarriers for the skin cancer delivery: *in vitro* evaluation. *J Liposome Res*. 2019; 29(3): 291-311. doi: 10.1080/08982104.2018.1556292, PMID 30526186.
- Hafez HN, El-Gazzar ABA. Synthesis and evaluation of antitumor activity of new 4-substituted thieno [3, 2-d]pyrimidine and thienotriazolopyrimidine derivatives. *Acta Pharm*. 2017; 67(4): 527-42. doi:10.1515/acph-2017-0039, PMID 29337675.
- Gürdere MB, Kamo E, Şahlın Yağlıoğlu AŞ, Budak Y, Ceylan M. Synthesis and *in vitro* anticancer evaluation of 1, 4-phenylene-bis-pyrimidine-2-amine derivatives. *Turk J Chem*. 2017; 41(2): 263-71. doi:10.3906/kim-1603-112.
- Kumar B, Sharma P, Gupta VP, Khullar M, Singh S, Dogra N, et al., Synthesis and biological evaluation of pyrimidine bridged combretastatin derivatives as potential anticancer agents and mechanistic studies. *Bioorg Chem*. 2018; 78: 13040. doi: 10.1016/j.bioorg.2018.02.027, PMID 29554587.
- Newman AC, Maddocks ODK. One-carbon metabolism in cancer. *Br J Cancer*. 2017; 116(12): 1499-504. doi:10.1038/bjc.2017.118, PMID 28472819.
- Saddik AA, Kamal El-Dean AM, El-Said WA, Hassan KM, Abbady MS. Synthesis, antimicrobial and anticancer activities of a new series of thieno [2, 3-d] pyrimidine derivatives. *J Heterocycl Chem*. 2018; 55(9): 2111-22. doi:10.1002/jhet.3256.
- Huang T, Wu X, Liu T, An L, Yin X. Synthesis and anticancer activity evaluation of novel oxacalix (2). *Med Chem Res*. 2019; 28(4): 580-90. doi:10.1007/s00044-019-02321-9.
- Liu YM, Chen CH, Yeh TK, Liou JP. Synthesis and evaluation of novel 7 H-pyrrolo-[2, 3-d] pyrimidine derivatives as potential anticancer agents. *Future Med Chem*. 2019; 11(9): 959-74. doi:10.4155/fmc-2018-0564.
- Ali SA, Awad SM, Said AM, Mahgoub S, Taha H, Ahmed NM. Design, synthesis, molecular modelling and biological evaluation of novel 3-(2-naphthyl)-1-phenyl-1H-pyrazole derivatives as potent antioxidants and 15-lipoxygenase inhibitors. *J Enzyme Inhib Med Chem*. 2020; 35(1): 847-63. doi:10.1080/14756366.2020.1742116, PMID 32216479.
- Veach DR, Namavari M, Beresten T, Balatoni J, Minchenko M, Djaballah H, et al., . Synthesis and *in vitro* examination of [124I]-, [125I]- and [131I]-2-(4-iodophenylamino) pyrido [2, 3-d] pyrimidin-7-one radiolabeled Abl kinase inhibitors. *Nucl Med Biol*. 2005; 32(4): 313-21. doi:10.1016/j.nucmedbio.2005.01.008, PMID 15878500.
- Marvaniya V, Joshi HV, Shah UA, Patel JK, Patel JR. Docking, synthesis and biological evaluation of pyridine ring containing diaryl urea derivatives as anticancer agents. *Int J Health Sci*. 2022; 3: 2851-65. doi:10.53730/ijhs.v6n53.6200.
- Galatage ST, Killedar SG, Katakara RB, Kumbhar RB, Sharma M, Shirote PJ. Development and characterization of floating tablets of nizatidine for peptic ulcer. *J Adv Med Pharm Sci*. 2020; 21(4): 1-12. doi:10.9734/jamps/2019/v21i430146.
- Galatage ST, Manjappa AS, Kumbhar PS, Salawi A, Sabei FY, Siddiqui AM, et al. Synthesis of silver nanoparticles using *Emilia sonchifolia* plant for treatment of bloodstream diseases caused by *Escherichia coli*. *Inann Pharm Fr Elsevier*. 2022.
- Galatage ST, Trivedi R, Bhagwat DA. Characterization of camptothecin by analytical methods and determination of anticancer potential against prostate cancer. *Future J Pharm Sci*. 2021; 7(1): 104. doi: 10.1186/s43094-021-00236-0.
- Galatage ST, Hebalkar AS, Gote RV, Mali OR, Killedar SG, Bhagwat DA, et al., Design and characterization of camptothecin gel for treatment of epidermoid carcinoma. *Future J Pharm Sci*. 2020; 6: 1.
- Galatage ST, Trivedi R, Bhagwat DA. Oral self-emulsifying nanoemulsion systems for enhancing dissolution, bioavailability and anticancer effects of camptothecin. *J Drug Deliv Sci Technol*. 2022; 78: 103929. doi: 10.1016/j.jddst.2022.103929.
- Kumbhar VM, Muddapur UM, Bhat KG, Shwetha HR, Kugaji MS, Peram MR, et al., Cancer stem cell traits in tumor spheres derived from primary laryngeal carcinoma cell lines. *Contemp Clin Dent*. 2021; 12(3): 247-54. doi: 10.4103/ccd.ccd_252_20, PMID 34759681.
- Ali HR, Naser AW. Synthesis, biological activity and molecular docking study of some new chalcones, pyrazolines and isoxazolines derivatives bearing 1, 2, 3-triazoline. *Int J Health Sci*. 2022; 6: Suppl 6: 76-118. doi: 10.53730/ijhs.v6n56.9173.
- Kumbhar VM, Muddapur U, Bin Muhsinah A, Alshehri SA, Alshahrani MM, Almazni IA, et al., Curcumin-encapsulated nanomicelles improve cellular uptake and cytotoxicity in cisplatin-resistant human oral cancer cells. *J Funct Biomater*. 2022; 13(4): 158. doi: 10.3390/jfb13040158, PMID 36278627.
- Gaeta R, Giuffra V, Fornaciari G. Cancer in the Renaissance court of Naples. *Lancet Oncol*. 2017; 18(8): e432. doi: 10.1016/S1470-2045(17)30464-3, PMID 28759378.
- Mohamed MM, Khalil AK, Abbass EM, El-Naggar AM. Design, synthesis of new pyrimidine derivatives as anticancer and antimicrobial agents. *Synth Commun*. 2017; 47(16): 1441-57. doi: 10.1080/00397911.2017.1332223.
- Kodoli RS, Galatage ST, Killedar SG, Pishwikar SA, Habbu PV, Bhagwat DA. Hepatoprotective activity of *Phyllanthus niruri* Linn. endophytes. *Future J Pharm Sci*. 2021; 7(1): 97. doi: 10.1186/s43094-021-00243-1.
- Nadaf SJ, Killedar SG. Curcumin nanocochleates: use of design of experiments, solid state characterization, *in vitro* apoptosis and cytotoxicity against breast cancer MCF-7 cells. *J Drug Deliv Sci Technol*. 2018; 47: 337-50. doi: 10.1016/j.jddst.2018.06.026.
- Kumbhar VM, Peram MR, Kugaji MS, Shah T, Patil SP, Muddapur UM, et al. Effect of curcumin on growth, biofilm formation and virulence factor gene expression of *Porphyromonas gingivalis*. *Odontology*. 2021; 109(1): 18-28. doi:10.1007/s10266-020-00514-y, PMID 32279229.
- Manjappa AS, Kumbhar PS, Patil AB, Disouza JI, Patravale VB. Polymeric mixed micelles: improving the anticancer efficacy of single-copolymer micelles. *Crit Rev Ther Drug Carrier Syst*. 2019; 36(1): 1-58. doi: 10.1615/CritRevTherDrugCarrierSyst.2018020481, PMID 30806205.
- Patil KS, Hajare AA, Manjappa AS, More HN, Disouza JI. Design, development, *in silico* and *in vitro* characterization of docetaxel-loaded TPGS/pluronic F 108 mixed micelles for improved cancer treatment. *J Drug Deliv Sci Technol*. 2021; 65: 102685. doi: 10.1016/j.jddst.2021.102685.
- Sambamoorthy U, Manjappa AS, Eswara BR, Sanapala AK, Nagadeepthi N. Vitamin E oil incorporated liposomal melphalan and simvastatin: approach to obtain improved physicochemical characteristics of hydrolysable melphalan and anticancer activity in combination with simvastatin against multiple myeloma. *AAPS PharmSciTech*. 2022; 23: 1-6.
- Galatage ST, Manjappa AS, Bhagwat DA, Trivedi R, Salawi A, Sabei FY, Alsalmi A. Oral self- nanoemulsifying drug delivery systems for enhancing bioavailability and anticancer potential of fosfestrol: *In vitro* and *in vivo* characterization. *Eur J Pharm BioPharma*. 2023; 193: 28-43 doi: 10.1016/j.ejpb.2023.10.013.
- Yadav V, Galatage ST, Manjappa AS, Salawi A, Peram MR, Nadaf SJ, Harale SS. Green Synthesis of silver nanoparticles from clematis gouriana leaf extract: Physicochemical characterization and antibacterial activity determination for treatment of blood stream infections. *The Microbe*. 2024: 100197.

Cite this article: Holam M, Galatage S, Gaud S, Kumbhar S, Devaru A, Inamdar S, et al. Molecular Docking, Synthesis and Determination of Anticancer Potential of Novel Pyrimidine Derivatives: *In vitro* and *in silico* Characterization. *Indian J of Pharmaceutical Education and Research*. 2026;60(1):361-73.